Axial Magnetic Fields in Relativistic Self-Focusing Channels

A. Kim,[1] M. Tushentsov,[1] D. Anderson,[2] and M. Lisak[2]

[1]*Institute of Applied Physics, Russian Academy of Sciences, 603950 Nizhny Novgorod, Russia*
[2]*Department of Electromagnetics, Chalmers University of Technology, SE-412 96 Göteborg, Sweden*

(Received 10 April 2002; published 8 August 2002)

Based on an improved cavitation model for the electron dynamics, an exact analysis is presented of the generation of axial magnetic fields in the relativistic self-focusing channels produced by circularly polarized light in plasmas. Two kinds of waveguiding structures are considered: single-channel waveguides and plasma filaments surrounded by a light field. It is found that due to large electron density gradients in the cavitation plasma, magnetic fields of megagauss values with opposite directions separated by a neutral sheet, where the magnetic field passes through zero, can be produced.

DOI: 10.1103/PhysRevLett.89.095003 PACS numbers: 52.35.Mw, 52.38.Fz

In recent years, the problem of the generation of strong magnetic fields has assumed an important role in the studies of superintense laser-plasma interaction [1–3]. This problem has both fundamental and application interests such as particle acceleration and inertial confinement fusion, as well as x-ray generation. In particular, increasing attention has been given to the generation of axial magnetic fields in an underdense plasma by high power circularly polarized lasers [4–7] with powers which frequently exceed the threshold level for relativistic self-focusing [8] and where self-channeling and cavitation phenomena play an exceptionally important role [9–11]. The importance of this phenomenon is not only intrinsic but is also related to the requirements of most of the advanced application schemes, e.g., inertial confinement fusion [12], where the laser radiation has to propagate over distances considerably beyond the diffraction limit. Numerical and experimental studies have given evidence for the formation of stable channels and radiation filaments [13,14].

As was shown by Sun *et al.* [9], the properties of relativistic self-focusing can change drastically for very high power beams. In this case, the laser intensity is so strong that the ponderomotive force can expel all electrons from the region of the high intensity field. The laser radiation is then confined in a self-induced waveguide, which is emptied of electrons already for laser powers slightly exceeding the threshold level, $P > 1.1P_{cr}$. Recent studies [11,14] demonstrated that stable channeling can occur with propagating power significantly exceeding the critical one for relativistic self-focusing, i.e., $P > P_{cr} = 17\omega^2/\omega_{pe}^2$ GW. However, as was pointed out in [14], these cavitation structures have nonzero global charge and, therefore, these and also subsequent works on magnetic field generation due to the inverse Faraday effect in the cavitation channel [15–17] deal with a model where plasma quasineutrality is violated. Recently, an improved cavitation model that allowed for exact quasisteady solutions describing the transverse structures of waveguide channels with electron cavitation was presented [18]. In this model both the ponderomotive and relativistic nonlinearities were taken into account including the constraint given by the total charge conservation. The main feature of the relativistic self-focusing channel in the cavitation regime, as seen from the point of view of magnetic field generation, lies in the large electron density gradients in the plasma region surrounding the vacuum (pure ion) channel that occurs due to the charge conservation constraint. In the present Letter, based on this model, we present an exact analysis of the axial magnetic field generation in the relativistic self-focusing channel produced by a circularly polarized light and show that the distribution has oppositely directed magnetic field regions of megagauss level divided by a narrow *neutral sheet* where the field is equal to zero. We pay particular attention to the neutral sheet because in this region, due to reconnection processes of magnetic field lines, anomalous dissipation of energy can take place (see, for example, [19]).

Let us consider the interaction between an underdense plasma and an ultrahigh power laser with comparatively long pulses so that the pulse width exceeds the electron oscillation time ($\tau \gg \omega_{pe}^{-1}$) but is less than the ion response time ($\tau \ll \omega_{pi}^{-1}$). This makes it possible to treat the ions as an immobile neutralizing background. Given the assumptions about the characteristic time scales of the interacting pulse and the plasma, we expect that stationary plasma-field structures can emerge, as the electron fluid should have time to approach a quasisteady state. The question if these structures actually appear on a time scale that effectively allows us to disregard other effects and complications was in fact confirmed by numerical simulations in [14]. In order to arrive at the well-known quasisteady model of relativistic self-focusing, we reduce the system of Maxwell's equations and the relativistic hydrodynamic equations describing the motion of a cold electron fluid by adopting the Coulomb gauge

$$\nabla \cdot \mathbf{A} = 0 \tag{1}$$

and representing the vector potential as a sum of quasistatic (low frequency) and high frequency parts, $\mathbf{A}(\mathbf{r}, t) = \langle \mathbf{A} \rangle (\mathbf{r}_\perp, z) + \mathrm{Re}\{A_\sim(\mathbf{r}_\perp, z)(\mathbf{e}_x + i\mathbf{e}_y) \exp[i(kz - \omega t)]\}$, where z is the propagation coordinate and $k = \omega/c$ is the

vacuum wave number. The equation for the quasistatic part of the potential can be taken in the form

$$\nabla^2\langle\mathbf{A}\rangle - \frac{4\pi e^2}{mc^2}\left\langle\frac{N}{\gamma}\right\rangle\langle\mathbf{A}\rangle = \frac{4\pi e^2}{mc^2}\left\langle\left(\frac{N}{\gamma}\right)_{\sim}\mathbf{A}_{\sim}\right\rangle, \quad (2)$$

where $\langle\ldots\rangle$ denotes averaging over the fast optical time scale, and $\gamma = (1 + e^2|\mathbf{A}|^2/m^2c^4)^{1/2}$ is the relativistic factor. Taking into account the Coulomb gauge (1), the continuity equation can be written as

$$\frac{\partial N}{\partial t} + \frac{e}{mc}\left(\mathbf{A}\cdot\nabla\frac{N}{\gamma}\right) = 0. \quad (3)$$

It should be emphasized that due to the inequality $\tau \gg \omega_{pe}^{-1}$, we can adopt a quasisteady model of self-channeling where the electron momentum can be assumed to be $\mathbf{p} = e\mathbf{A}/c$, if the generalized vorticity was zero before the arrival of the laser pulse (see, for example, [20]). For the high frequency part we arrive at the following relativistic self-focusing equations in the paraxial approximation:

$$2ik\frac{\partial A_{\sim}}{\partial z} + \nabla_{\perp}^2 A_{\sim} - \frac{k^2 N_0}{\langle\gamma\rangle}\langle N\rangle A_{\sim} = 0, \quad (4)$$

$$\nabla_{\perp}^2\varphi = 4\pi e(\langle N\rangle - N_0), \quad (5)$$

$$\varphi/mc^2 = \langle\gamma\rangle - 1 \quad \text{if } \langle N\rangle \neq 0, \quad (6)$$

where $\langle\gamma\rangle = (1 + e^2|A_{\sim}|^2/m^2c^4)^{1/2}$, $\nabla_{\perp}^2 \equiv \partial^2/\partial x^2 + \partial^2/\partial y^2$, φ is the scalar quasistatic potential, and we have also introduced low and high frequency parts for the electron density, $N = \langle N\rangle + N_{\sim}$. However, as can be seen from Eq. (3), which expresses the charge conservation law that for quasistatic motion implies a requirement on the vector character of the field only; i.e., for example, in the axisymmetric case the quasistatic vector potential has only an azimuthal component, $\langle\mathbf{A}\rangle = A_{\varphi}\mathbf{e}_{\varphi}$. Consequently, the quasistatic magnetic field, which is defined directly from the definition of the vector potential,

$$\langle\mathbf{B}\rangle = \nabla\times\langle\mathbf{A}\rangle, \quad (7)$$

is oriented along the direction of propagation z, $\langle\mathbf{B}\rangle = B\mathbf{e}_z$, where $B = (1/r)[d(rA_{\varphi})/dr]$. In Eqs. (4)–(6), we can neglect the influence of the generated magnetic field, since the corresponding gyrofrequency is much smaller than the carrier frequency. The equations have to be solved self-consistently along with the constraint given by total charge conservation; i.e., the integral over the whole plasma space of the right hand of Eq. (5) must be equal to zero:

$$\int_{-\infty}^{\infty}(\langle N\rangle - N_0)d\mathbf{r} = 0. \quad (8)$$

If this constraint is not fulfilled, self-focusing structures, even in simulations based on Eqs. (4)–(6), will not satisfy the quasineutrality condition [14].

Finally, using the high frequency part of Eq. (3), we can close Eq. (2) with the self-consistent set of Eqs. (4)–(6) and (8). For axisymmetric plasma-field structures, homogeneous along the propagation path, and assuming a laser field in the form $eA_{\sim}(\mathbf{r}_{\perp}, z)/mc^2 = a_s(r)\exp(-i\kappa z)$, the normalized vector potential $a_{\varphi} = eA_{\varphi}/mc^2 n_0^{1/2}$ obeys the following equation:

$$\Delta_r a_{\varphi} - \frac{1}{r^2}a_{\varphi} - \frac{n_s}{\gamma_s}a_{\varphi} = -\frac{a_s^2}{2\gamma_s}\frac{d}{dr}\left(\frac{n_s}{\gamma_s}\right). \quad (9)$$

Here $\Delta_r \equiv (1/r)d(rd/dr)/dr$, $\gamma_s = (1 + a_s^2)^{1/2}$, $n_0 = N_0/N_c$, and we have used the following dimensionless variables: $r = k\sqrt{n_0}r$ and $z = kn_0 z/2$. In these variables, Eqs. (4)–(6) can be rewritten as

$$\Delta_r a_s + \left(\kappa - \frac{n_s}{\gamma_s}\right)a_s = 0, \quad (10)$$

$$\Delta_r\phi_s = n_s - 1, \quad (11)$$

$$\phi_s = \gamma_s - 1 \quad \text{in the region where } n_s(r) \neq 0. \quad (12)$$

Thus the solutions of Eq. (9) depend on the power $\tilde{P} = \int_0^{\infty} a_s^2 r dr$ only or in real parameters they depend on the relation of laser power over the critical one for relativistic self-focusing: P/P_{cr}. Here $n_s = \langle N\rangle/N_0$, $\phi_s = \varphi/mc^2$, and κ is the propagation constant that must be considered as an eigenvalue for the corresponding localized eigenfunctions: $a_s(r), \phi_s(r) \to 0$, $n_s(r) \to 1$ at $r \to \infty$ [18]. It should be noted that when calculating the magnetic field, Eq. (9) must also be considered within the class of functions for $B(r)$ which vanish at infinity, $B(r) \to 0$. Thus, the distribution of the axial magnetic field and its value in the self-focusing channel are defined by these variables as

$$B = B_o n_0 \frac{1}{r}\frac{d(ra_{\varphi})}{dr} = B_o n_0 \Omega(r, P/P_{cr}); \quad (13)$$

($B_o = mc\omega/e$) depends on two parameters: the background plasma density n_0 and the laser power trapped in the waveguide, i.e., P/P_{cr}. Here the function $\Omega(r, P/P_{cr})$ can be viewed as a universal function characteristic of the kind of self-channeling structures. We emphasize that the sources (azimuthal macroscopic current) of axial magnetic field generation are electron density and/or laser intensity inhomogeneities as follows from the right-hand side of Eq. (9) since space charge rotating in the azimuthal direction in a circularly polarized light can be produced only by a plasma inhomogeneity (see, for example, [21]) or an intensity inhomogeneity. In the cavitation channels, the main contribution comes from the electron inhomogeneity due to their large gradients, which are able to significantly modify the magnetic field distribution. Next we consider two examples of relativistic self-focusing structures that may represent situations of practical interests.

Single-channel waveguiding.—We start with the most important solutions describing single-channel waveguide structures. These structures are stable, in spite of the fact that they guide laser powers significantly exceeding the self-focusing power, $P \gg P_{cr}$, and can be produced in relativistic laser pulse interaction with plasmas. The

improved cavitation model of relativistic self-focusing suggested in Ref. [18] makes it possible to calculate waveguide structures which are consistent with the constraint of global charge quasineutrality. The idea is that, as follows from Eq. (12), the solutions of Eqs. (10)–(12) in the cavitation ($n_s = 0$ at $r < R$) and noncavitation ($n_s \neq 0$ at $r \geq R$) regions must be considered separately and their matching must be done in accordance with the integral constraint (8). Examples of such solutions for $P/P_{cr} =$ 1.07, 1.4, and 44 are shown in Fig. 1. An attractive peculiarity of such self-channeling structures from the point of view of axial magnetic field generation is that the interplay between the relativistic ponderomotive force expelling electrons from the cavitation channel and the electrostatic force due to charge separation leads to electron density distributions with large gradients. Within this model, the density profile immediately adjacent to the cavity may look like a jump, i.e., $n_s(R) \neq 0$, which means that large azimuthal surface currents can be generated on the boundary of the channel. The density gradients in the deep region ($r > R$) may have a reversed sign which gives rise to an oppositely directed microscopic current. These two currents can result in the production of a magnetic field distribution with oppositely directed fields of the same order of magnitudes [see Figs. 1(b) and 1(c)]. For a given solution of Eqs. (10)–(12), i.e., $n_s(r)$ and $a_s(r)$, Eq. (9) determines the axial magnetic field and we solve the equations numerically by using the shooting method to get a localized solution for $B(r)$. In order to do this, we use the vacuum solution of Eq. (9) in the cavitation region ($r < R$): $a_\varphi = \Omega_{ch} r/2 \equiv B_{ch} r/2B_o n_0$, where the magnetic field is homogeneous, $B \equiv B_{ch} = \text{const}$ and $\Omega \equiv \Omega_{ch}$. In the noncavitation region, Eq. (9) must be supplemented with boundary conditions, where one of them is obtained from the continuity of the vector potential, i.e., $a_\varphi(R) = \Omega_{ch} R/2$. Another condition on the first derivative can be obtained by integrating Eq. (9) over the boundary at $r = R$:

$$a'_\varphi(R) = \frac{1}{2}\Omega_{ch} - \left[\frac{a_s^2}{2\gamma_s^2} n_s\right]_{r=R}. \tag{14}$$

Here Ω_{ch} must be considered as a shooting parameter. Results of the calculations are presented in Fig. 2 in the form of functions $\Omega_{ch}(P/P_{cr})$ and $\Omega_m(P/P_{cr})$ that correspond to the axial magnetic field in the vacuum channel $r < R$ and the maximum of the oppositely directed magnetic field in the plasma region, respectively. When $P \gg P_{cr}$, the oppositely directed magnetic field reaches its maximum value very near the cavitation boundary $r = R$, so the neutral sheet is extremely narrow and located close to the cavity.

Based on our calculations, we present estimates corresponding to a $\lambda = 1$ μm laser with power $P = 30$ TW and plasma density $N_0 = 2.8 \times 10^{19}$ cm^{-3}. In this case $P/P_{cr} \simeq 44$, the radius of the cavitation channel is $R =$ 3.8 μm and the magnetic field distribution is as in Fig. 1(c) with a magnetic field in the channel $B_{ch} \simeq 1.1$ MG and the oppositely directed magnetic field $B_m = B_o n_0 \Omega_m \simeq -3.7$ MG. It should be noted that the self-channeling plasma-field structures and therefore the axial magnetic field depend on integral characteristics such as trapped laser power in the channel, while the ''vacuum focusable intensity'' influences rather the possibility of excitation of these structures and their transient length of excitation. Although these structures, even with $P \gg P_{cr}$, are stable against small perturbations, the transient stage, where filamentation instability can occur leading to the formation of a number of single channels with $P \sim P_{cr}$, depends on the geometry of the interaction.

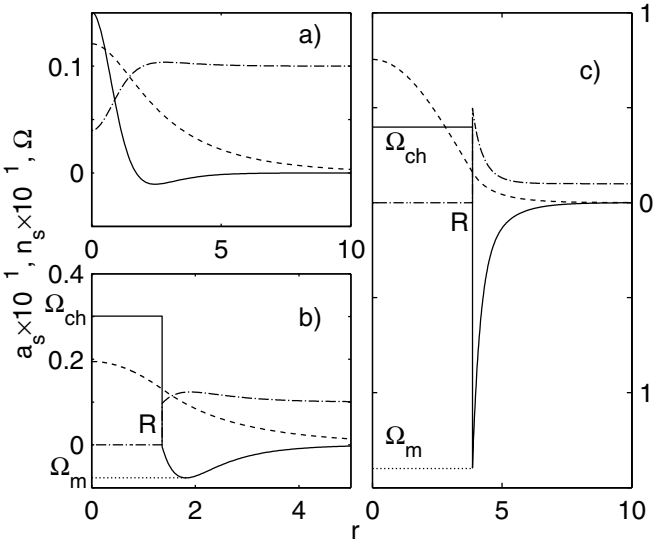

FIG. 1. Single-channel structures with corresponding magnetic field distributions for $P/P_{cr} = 1.07$ (a), 1.4 (b), and 44 (c): electron density (dash-dotted line), field (dashed line), and magnetic field (solid line) distributions.

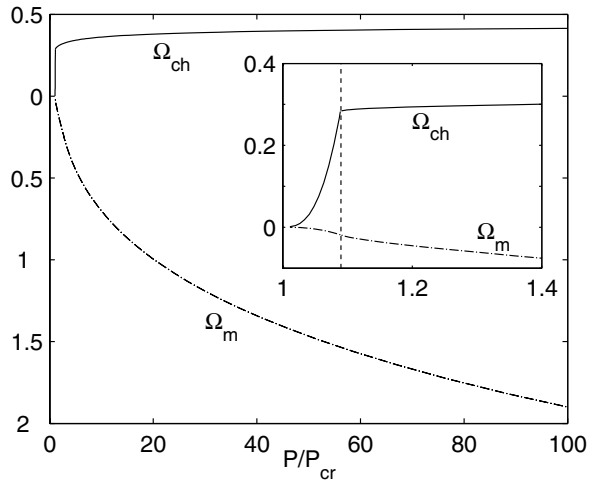

FIG. 2. Dependence of the magnetic field in the cavity, Ω_{ch} (solid line), and the maximum of the oppositely directed magnetic field in the plasma region, Ω_m (dash-dotted line), on the laser power. The inset shows curves in detail at powers near the critical one.

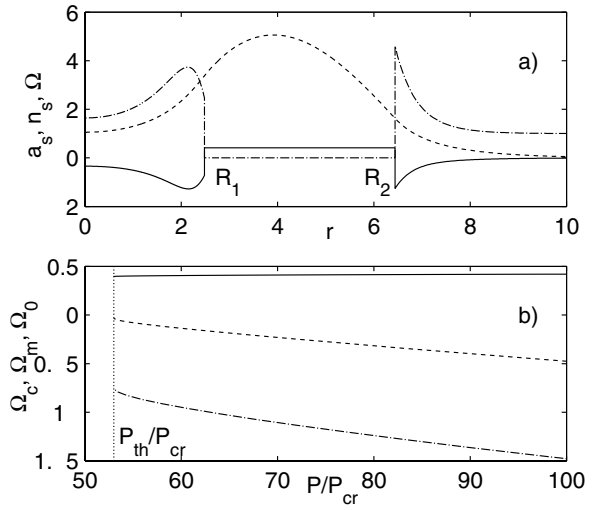

FIG. 3. (a) Structure of plasma filament surrounded by field with corresponding magnetic field distribution for $P = 82P_{cr}$: electron density (dash-dotted line), field (dashed line), and magnetic field (solid line) distributions. (b) Dependence of the magnetic field on the axis, Ω_0 (dashed line), the maximum of the magnetic field in the plasma filament, Ω_m (dash-dotted line), and the magnetic field in the vacuum channel, Ω_c (solid line), on the laser power.

Plasma filament surrounded by a laser field.—Another relativistic self-focusing structure that can be of interest for applications is a plasma filament surrounded by a ring-shaped laser field [18]. An example of such structures where a central plasma filament with high electron density is supported by a strong laser field is shown in Fig. 3(a). These solutions exist only in the cavitation regime where multifilament self-focusing structures are also possible, and they are stable if the laser power exceeds the threshold level, $P > P_{th} = 53P_{cr}$. Since large azimuthal currents generated on the boundaries R_1 and R_2 have opposite directions, for these structures we can also expect large magnetic field generation in the plasma filament and oppositely directed magnetic fields in the surrounding vacuum channel. The procedure to calculate the magnetic field for a given plasma-filament structure is as follows: shooting from the central axis $r = 0$ of the filament with the initial conditions $a_\varphi(0) = 0$ and $a'_\varphi(0) = b$, where b is a shooting parameter, we find the solution for the magnetic field and calculate $a_\varphi(R_1)$ and $a'_\varphi(R_1)$ at the boundary R_1. Then, making use of the vacuum solution, $a_\varphi = \Omega_c r/2 +$ const, of Eq. (9) with matching vector potential a_φ and its first derivative a'_φ on the boundary R_1, we arrive at the boundary R_2, where the boundary conditions are

$$a_\varphi(R_2) = a_\varphi(R_1) + (R_2 - R_1)\left[a'_\varphi + \frac{a_s^2}{2\gamma_s^2} n_s\right]_{R_1}, \quad (15)$$

$$a'_\varphi(R_2) = a_\varphi(R_1) + \left[\frac{a_s^2}{2\gamma_s^2} n_s\right]_{R_1} - \left[\frac{a_s^2}{2\gamma_s^2} n_s\right]_{R_2}. \quad (16)$$

Now we can continue by solving Eq. (9) to get the magnetic field distribution in all space, requiring that $B(r) \to 0$ as $r \to \infty$. Results are shown in Fig. 3 as the magnetic field distribution for $P/P_{cr} = 82$ (a), and in (b) as the magnetic field on the axis, $\Omega_0 = \Omega(r = 0)$, the maximum of the magnetic field in the plasma filament Ω_m vs P/P_{cr}, and $\Omega_c(P/P_{cr})$ that defines the magnetic field in the vacuum channel $R_1 < r < R_2$ as $B_c = B_o n_0 \Omega_c$.

In conclusion, we have presented an exact analysis of axial magnetic field generation in plasma channels produced by circularly polarized light with relativistic intensities. The main consequence of this work is that, at laser powers higher than the relativistic self-focusing one, distributions of oppositely directed magnetic fields with field strengths of the order of megagauss and separated by a neutral sheet (a region where the field passes through zero) can be produced in the plasma channel.

[1] S. C. Wilks *et al.*, Phys. Rev. Lett. **69**, 1383 (1992).
[2] A. Pukhov and J. Meyer-ter-Vehn, Phys. Rev. Lett. **76**, 3975 (1996).
[3] R. J. Mason and M. Tabak, Phys. Rev. Lett. **80**, 524 (1998).
[4] Y. Horovitz *et al.*, Phys. Rev. Lett. **78**, 1707 (1997).
[5] Z. Najmudin *et al.*, Phys. Rev. Lett. **87**, 215004 (2001).
[6] M. G. Haines, Phys. Rev. Lett. **87**, 135005 (2001).
[7] I.Yu. Kostyukov *et al.*, Laser Part. Beams **19**, 133 (2001).
[8] A.G. Litvak, Sov. Phys. JETP **30**, 344 (1970); C. Max, J. Arons, and A. Langdon, Phys. Rev. Lett. **33**, 209 (1974); P. Sprangle, C. M. Tang, and E. Esarey, IEEE Trans. Plasma Sci. **15**, 145 (1983).
[9] G. Z. Sun, E. Ott, Y. C. Lee, and P. Guzdar, Phys Fluids **30**, 526 (1987).
[10] T. Kurki-Suonio, P. J. Morrison, and T. Tajima, Phys. Rev. A **40**, 3230 (1989).
[11] A. B. Borisov *et al.*, Phys. Rev. Lett. **68**, 2309 (1992); Phys. Rev. A **45**, 5830 (1992).
[12] M. Tabak *et al.*, Physics of Plasmas **1**, 1626 (1994).
[13] M. Borghesi *et al.*, Phys. Rev. Lett. **78**, 879 (1997); K. A. Tanaka *et al.*, Phys. Rev. E **62**, 2672 (2000).
[14] M. D. Feit *et al.*, Phys. Rev. E **57**, 7122 (1998).
[15] Z. M. Sheng and J. Meyer-ter-Vehn, Phys. Rev. E **54**, 1833 (1996).
[16] V. I. Berezhiani, S. M. Mahajan, and N. L. Shatashvili, Phys. Rev. E **55**, 995 (1997).
[17] T. Lehner and L. di Menza, Phys. Rev. E **65**, 016414 (2002).
[18] A. Kim *et al.*, Phys. Rev. E **65**, 036416 (2002); F. Cattani *et al.*, Phys. Rev. E **64**, 016412 (2001).
[19] A.A. Galeev, in *Basic Plasma Physics II*, edited by A. A. Galeev and R. N. Sudan (North-Holland, Amsterdam, 1984), p. 305.
[20] X. L. Chen and R. N. Sudan, Phys. Fluids B **5**, 1336 (1993).
[21] L. Gorbunov, P. Mora, and T. M. Antonsen, Jr., Phys. Rev. Lett. **76**, 2495 (1996); L. M. Gorbunov and R. R. Ramazashvili, Sov. Phys. JETP **87**, 461 (1998).